Evaporation-cost dependence in heavy-ion fragmentation

L. Audirac,[1] A. Obertelli,[1] P. Doornenbal,[2] D. Mancusi,[1] S. Takeuchi,[2] N. Aoi,[3] H. Baba,[2] S. Boissinot,[1] A. Boudard,[1] A. Corsi,[1] A. Gillibert,[1] T. Isobe,[2] A. Jungclaus,[4] V. Lapoux,[1] J. Lee,[2] S. Leray,[1] K. Matsui,[5] M. Matsushita,[6,7] T. Motobayashi,[2] D. Nishimura,[8] S. Ota,[6] E.C. Pollacco,[1] G. Potel,[1] H. Sakurai,[2,5] C. Santamaria,[1] Y. Shiga,[7] D. Sohler,[9] D. Steppenbeck,[6] R. Taniuchi,[5] and H. Wang[2,10]

[1]*CEA, Centre de Saclay, IRFU/Service de Physique Nucléaire, F-91191 Gif-sur-Yvette, France*
[2]*RIKEN Nishina Center, 2-1 Hirosawa, Wako, Saitama 351-0198, Japan*
[3]*Research Center for Nuclear Physics, Osaka University, Ibaraka, Osaka 567-0047, Japan*
[4]*Instituto de Estructura de la Materia, CSIC, E-28006 Madrid, Spain*
[5]*Department of Physics, University of Tokyo, 7-3-1 Hongo, Bunkyo, Tokyo 113-0033, Japan*
[6]*Center of Nuclear Study, University of Tokyo, RIKEN campus, 2-1 Hirosawa, Wako, Saitama 351-0298, Japan*
[7]*Department of Physics, Rikkyo University, 3-34-1 Nishi-Ikebukuro, Toshima, Tokyo 172-8501, Japan*
[8]*Department of Physics, Tokyo University of Science, Noda, Chiba 278-8510, Japan*
[9]*MTA Atomki, P.O. Box 51, H-4001 Debrecen, Hungary*
[10]*State Key Laboratory of Nuclear Physics and Technology, Peking University, Beijing 100871, P.R. China*

Inclusive multi-neutron and multi-proton removal cross sections from ^{112}Sn and ^{104}Sn at relativistic energies have been measured. The data show two distinct regimes of the reaction process depending on the nucleon evaporation cost of the final nucleus. This behaviour is universal regarding the mass or asymmetry of the initial system or target composition. A state-of-the-art cascade and de-excitation model reproduces the observed trend but systematically fails in reproducing cross sections for the removal of the more bound nucleon species.

PACS numbers:

The fragmentation of a many-body bound system from the fast collision with an extra particle is a generic problem in areas as different as atomic physics through electron-induced ionization [1], nuclear physics through the nuclear fragmentation in spallation targets [2] or astrophysics through the ejection of rocks from gravitational rings after asteroid collisions [3]. This complex process depends *a priori* on the two-body interaction cross section, the geometry of the system and the binding of its individual constituents. This multi-particle removal probability is challenging to predict to a high precision since it also depends on processes such as re-interaction of scattered components and release of dissipation energy by statistical emission of particles, *e.g.*, the ionization of atoms by energetic electrons is impacted by the Auger effect. Models for nuclear fragmentation have been numerous [4]. At kinetic energy larger than 100 MeV/nucleon, it is possible to accurately reproduce experimental fragmentation cross sections by modeling the reaction in two steps: intra-nuclear cascade (INC) followed by statistical de-excitation of the remnant nucleus [2]. Fragmentation results from the interplay of both processes [5]. In the case of one-nucleon removal, the proton-neutron asymmetry has recently demonstrated important limits of our treatment of direct reactions [6, 7] and the role of evaporation in weakly bound nuclei has been questioned for deeply-bound nucleon removal [8]. In this rapid communication, we present new fragmentation data from stable and unstable Sn isotopes at incident energies of ∼165 MeV/nucleon. We characterize these data by the difference in emission cost between the removed species and the other one, $\Delta C = C_{\rm removed} - C_{\rm other}$, where $C_n = S_n$ is the neutron-evaporation cost, $C_p = S_p + V_c$ is the proton-evaporation cost, $S_{n(p)}$ is the neutron (proton) separation energy and V_c is the Coulomb barrier. We show that the ejection of identical nucleons presents two universal regimes depending on the sign of ΔC.

Fast ^{104}Sn and ^{112}Sn beams at respectively 155 and 173 MeV/nucleon have been produced at the RIBF facility, operated conjointly by the RIKEN Nishina Center and the CNS of the University of Tokyo, by fragmentation of a ^{124}Xe primary beam of 0.5 eμA onto a 0.555 g/cm^2 ^{9}Be production target. The secondary cocktail beams were composed of ^{104}Sn (^{112}Sn) at 25% (77%) purity. The achieved intensity of ^{104}Sn was 350 pps. Secondary targets were located at the F8 focal point of the BigRIPS spectrometer [9, 10]. Cross sections were measured from 2-mm thick ^{12}C and CH_2 targets. The target thicknesses were determined with a 2% precision by both weighting and magnetic-rigidity deviation of the beam in the zero-degree spectrometer (ZDS) after energy loss in the secondary target. The direct beam and reaction products were transmitted to the F11 focal plane through the large acceptance of the ZDS, namely ±4% in momentum and 5 msr in angle. Hydrogen induced cross sections have been deduced from the CH_2 target measurements after subtraction of the measured carbon contribution. Beam particles (secondary products) were identified with BigRIPS (ZDS) by means of the $B\rho - \Delta E - TOF$ method with the use of beam-tracking detectors, plastic detectors and ionization chambers for beam position, time of flight and energy-loss measurements, respectively. After the

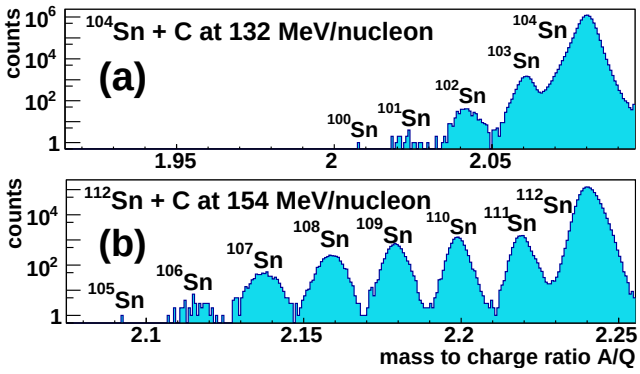

FIG. 1: (Color online) Mass identification of fully-stripped tin isotopes from the fragmentation of incoming ^{104}Sn (a) and ^{112}Sn (b).

secondary target, several charge states (84%, 15%, 1% for $Q = +50, +49, +48$, respectively) were observed for the outgoing ions. Ions with no charge-state change between the secondary target and the ZDS focal plane were selected in the analysis. Several factors were considered to correct the number of detected products and to extract the production cross sections: (*i*) the ZDS momentum acceptance, (*ii*) contamination of charge states of lower-mass isotopes, (*iii*) detection efficiency of tracking detectors and ionization chambers (94%), (*iv*) the charge state conservation between the secondary target and the focal plane of the ZDS (70(2)%), (*v*) the absorption of beam-like particles with tracking-detector material upstream and downstream the secondary target (6%), (*vi*) spurious contribution to the measured cross section from interaction with beam scintillators (17%). A mass resolution of $\sigma \sim 10^{-3}$ for the residues transmitted through the ZDS was achieved, allowing a clean separation of reaction products (see Fig. 1) for isotopes from the neutron removal from ^{104}Sn and ^{112}Sn. Different Bρ magnetic rigidity settings of the ZDS were used. The resulting measured cross sections are shown in Table I. The uncertainties quoted in Tab. I are taken as the quadratic sum of all sources of uncertainties.

The removal cross sections as a function of the number of removed nucleons and normalized to the one-nucleon removal cross section are shown in Fig. 2. Our data highlight two behaviours: neutron removal from the neutron-deficient ^{104}Sn presents a steep slope as a function of the number of removed neutrons, whereas the few-neutron removal from the stable ^{112}Sn exhibits a much flatter slope with a steeper slope beyond five removed neutrons. Comparison with the literature demonstrates that our data sets are actually prototypes of two general classes. Proton removal from the very neutron-rich ^{132}Sn [11],^{136}Xe [12] at 1 GeV/nucleon or neutron removal from the neutron-deficient ^{58}Ni [13] at 650 MeV/nucleon superimpose to the ^{104}Sn data obtained from neutron removal, whereas neutron removal from ^{132}Sn behaves like neutron removal from ^{112}Sn. Surprisingly enough, other nucleon-removal cross sections from Ca, Se and Pb [14–16] at incident energies ranging from 140 MeV/nucleon to 1 GeV/nucleon show exactly the same tendency as shown in Fig. 2 and Fig. 3. The transition between these two regimes is illustrated by the neutron removal data from ^{112}Sn taken from this work and at GSI [17]. The GSI data set ranges from three-neutron removal to twelve-neutron removal, leading to the production of the dripline isotope ^{100}Sn. In Fig. 2, the GSI data are normalized to the three-neutron removal cross section from the present ^{112}Sn data since the one and two neutron removal cross sections have not been measured. The data do not present a unique slope as all other distributions but a transition from a flat to a steep behaviour. The relevant isotopes are associated with values of ΔC in the range between -15 and $+15$ MeV; the associated cross sections indeed exhibit a change of slope in the vicinity of $\Delta C = 0$ (see Fig. 3).

These two behaviours can be interpreted as consequences of the different role played by evaporation in the two ΔC regimes. We assume that evaporation always selects the "cheaper" species (i.e. protons if $C_p < C_n$, neutrons otherwise). In the following, ΔC is calculated from tabulated nucleon separation energies [18] and the Bass prescription [19, 20] for the Coulomb barrier. Under this assumption, removal of the "expensive" nuclear species (e.g. protons from ^{132}Sn, neutrons from ^{104}Sn) can never occur by evaporation; therefore, it *must* take place during the cascade stage *and* little excitation energy must

Proj.	Chan.	S_n	S_p	V_C	ΔC	σ expt (mb)		σ theory (mb)	
			(MeV)						
Target:						^{12}C	H	^{12}C	H
^{112}Sn	-1n	8.2	7.0	4.8	-3.6	151(7)	137(7)	180	132
	-2n	11.1	6.7	4.8	-0.3	98(4)	107(7)	92	109
	-3n	8.6	5.9	4.8	-2.1	59(3)	70(4)	38	64
	-4n	11.4	5.8	4.8	+0.8	26(1)	28(2)	22	49
	-5n	8.9	5.3	4.8	-1.2	5.1(9)	4.3(7)	6	17
	-6n	11.8	5.4	4.8	+1.5	0.4(2)	0.5(2)	3	8
	-1p	10.0	5.7	4.6	+0.4	51(5)	34(3)	105	41
	-2p	9.6	8.8	4.6	+3.7	5(1)	4(1)	14	2
^{104}Sn	-1n	10.0	4.3	4.8	+0.9	55(2)	51(4)	125	111
	-2n	13.4	4.1	4.8	+4.4	2.1(1)	2.6(3)	19	16
	-3n	11.2	3.5	4.8	+2.9	0.11(3)	0.12(4)	6	1.6
	-4n	17.3	3.0	4.8	+9.4	$0.006^{(+6)}_{(-4)}$	-	2	0.08
	-1p	11.9	3.1	4.7	-4.0	121(5)	70(7)	157	67
	-2p	11.5	5.4	4.6	-1.5	90(6)	58(7)	63	38
	-3p	11.2	3.9	4.5	-2.8	56(5)	33(7)	24	16
	-4p	11.0	6.8	4.4	+0.2	37(6)	-	10	6

TABLE I: Incoming nuclei, reaction channels and nucleon removal cross sections for both ^{12}C and H targets at mid-target energies of 132 (154) and 142 (161) MeV/nucleon for ^{104}Sn (^{112}Sn), respectively. Theoretical predictions from INCL-ABLA calculated at 150 MeV/nucleon are also given.

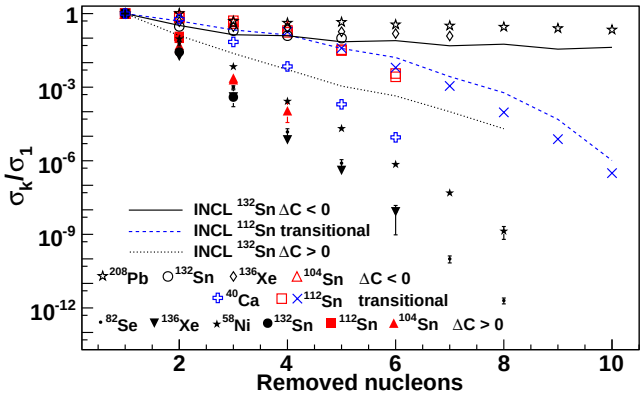

FIG. 2: (Color online) Inclusive multi-neutron (proton) removal cross sections normalized to the one-neutron (proton) removal cross section. Data for ^{104}Sn (triangles) and ^{112}Sn isotopes (squares) from this work are shown in red. Data for ^{132}Sn (circles) [11] at 950 MeV/nucleon, ^{136}Xe (open diamonds and filled black triangles) [12] at 1 GeV/nucleon, ^{58}Ni (filled stars) [13] at 650 MeV/nucleon, ^{40}Ca (blue open crosses) [14] and ^{82}Se (dots) [15] at 140 MeV/nucleon, ^{208}Pb (open stars) [16] and ^{112}Sn (blue crosses) [17] at 1 GeV/nucleon are shown. Filled (open) symbols represent the removal of the expensive (cheap) nucleon species. Selected INCL-ABLA calculations are plotted (lines).

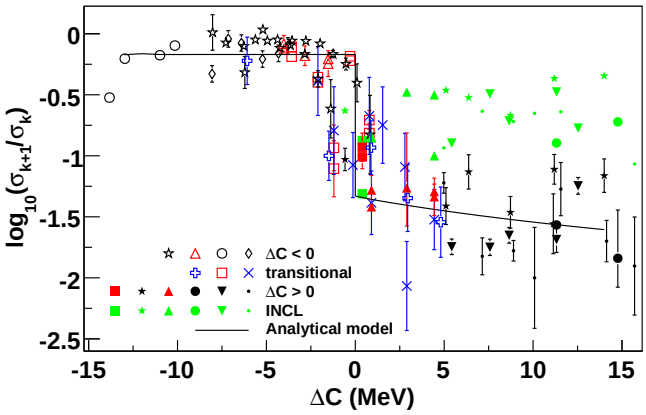

FIG. 3: (Color online) Ratio of the $k+1$ nucleon- and the k nucleon-removal cross sections in decimal logarithmic scale as a function of the evaporation cost asymmetry ΔC. The same notation as in Fig. 2 is used for markers. INCL calculations for the removal of the expensive nucleon species (green markers) and calculations of the analytical model (line) are shown.

be available at the beginning of evaporation, otherwise the competing nuclear species will be evaporated. In this regime ($\Delta C > 0$), evaporation acts like a cutoff in excitation energy: only cascade events with small energy deposit in the residual nucleus will contribute to the n-nucleon-removal cross section. An analogous mechanism contributes to the removal of the "cheap" nuclear species (e.g. neutrons from ^{132}Sn, protons from ^{104}Sn); however, it is also possible in this regime ($\Delta C < 0$) that part of the nucleons are removed during the evaporation phase, provided that the correct amount of excitation energy is available at the beginning of de-excitation. The dependence on the evaporation-cost asymmetry ΔC is illustrated in Fig. 3 where the derivative of the nucleon removal cross sections with respect to the number of removed nucleons is plotted as a function of ΔC, for all data sets shown in Fig. 2. The two regimes depend on the sign of ΔC. The observed generality of the ΔC regimes should be connected with the universality of the evaporation corridor [21], i.e. the locus of nuclides which evaporate protons and neutrons with equal probability.

We propose here a simplified scheme, in the same spirit as the cold fragmentation model [22], to capture the essence of the two regimes depicted in Fig. 2 and Fig. 3. We assume that (i) the ejection of one nucleon by INC results in an exponential excitation-energy distribution, $f_1(E) = e^{-E/T}/T$, where T is the mean value of the distribution; (ii) the excitation energy associated with the removal of k nucleons during INC is the sum of independent excitation energies deposited by each nucleon removal, which yields the distribution $f_k(E) = (E/T)^{k-1}/(k-1)! \times e^{-E/T}/T$; and finally, (iii) the cross section $\sigma_k^{\rm INC}$ for ejecting k nucleons during INC follows an exponential law such that $\sigma_{k+1}^{INC}/\sigma_k^{INC} = \alpha$. According to the above arguments, removal of k expensive nucleons, e.g. neutrons from ^{104}Sn, is only possible if they are all removed during the cascade. The cross section for this process is $\sigma_k^n = \sigma_k^{\rm INC} \int_0^{C_p} f_k(E){\rm d}E$. On the other hand, the removal of k cheap nucleons, e.g. protons from ^{104}Sn, originates in $j \leq k$ cascade and $k-j$ evaporations, following the sum over all possibilities $\sigma_k^p = \sum_{j=1}^{j=k} \sigma_j^{\rm INC} \int_{(k-j)C_p}^{(k-j+1)C_p} f_j(E){\rm d}E$. Formulas for neutron-rich residues are obtained by exchanging the n and p labels. Considering $\langle C_p \rangle = 10$ MeV, the numerical solution of the model for neutron removal from ^{132}Sn with (T=20 MeV,α=0.5) is shown on Fig. 3. The model parameters were fixed by comparison with the predictions of the intranuclear-cascade code described below. This simple model already shows a much steeper slope for the removal of the expensive species than for the cheap one. To go beyond this intuitive description of the reaction process, we compare our data to predictions from state-of-the-art calculations based on Monte-Carlo description of the cascade and evaporation processes. We use the Liège Intranuclear Cascade model (INCL), first developed at Liège by J. Cugnon and further developed at CEA-Saclay [23, 24]. The latest version of the code can simulate reactions on light nuclei up to $A = 18$ [25]. At the end of the cascade, the remnant nucleus is left with some excitation energy, subsequently released via evaporation of nucleons and light charged particles. In the present study, evaporation is simulated by the ABLA07 code [26]. INCL-ABLA yields the correct slope of the

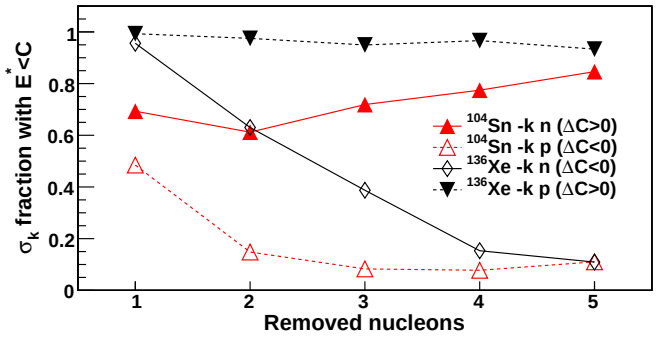

FIG. 4: (Color online) INC calculations of the fraction of the removal cross section σ_k for events whose intrinsic excitation energy $E^\star$ of the cascade remnant is below the evaporation cost C of the cheapest species.

multi-nucleon-removal curves for the cheap species, but systematically underestimates the magnitude of the slope for the expensive species (see Fig. 2 and Fig. 3). In the case of neutron removal from ^{104}Sn, we have verified that the slope is essentially insensitive to (*i*) ±20% isoscalar variations of the radius and diffusiveness parameters of the INCL Woods-Saxon densities, (*ii*) isovector variations of 0.2 fm for the same parameters (which simulate the presence of a neutron/proton skin), (*iii*) 50% variations of the level-density parameter in evaporation. The slope is sensitive to the proton Coulomb barrier, as predicted by the analytical model above and confirmed by the INC-evaporation calculations; however, the disagreement with the experimental slope cannot be cured by modifying the proton Coulomb barrier alone. Indeed, an increase of 1 MeV of the barrier for Sn isotopes increases $\log(\sigma^n_{k+1}/\sigma^n_k)$ by about 10%; however, it simultaneously induces a similar variation in the opposite direction in $\log(\sigma^p_{k+1}/\sigma^p_k)$, thereby degrading the agreement with the data. Moreover, the cross section slopes are sensitive to the proton barrier only if protons are the cheap species.

The underestimate of the magnitude of the slope can be traced back to a particular class of events: Fig. 4 shows which fraction of the cross section for the removal of k nucleons is due to a remnant whose intrinsic excitation energy is lower than its evaporation threshold (the smaller of the proton and neutron costs). These remnants cannot evaporate any particle and de-excite by gamma emission. The mispredicted cross sections ($\Delta C > 0$) are dominated by such events, which corroborates the basic assumptions of our simple analytical model (see above). Therefore, one might suspect that INC overestimates the frequency of such low-excitation events. The observed strong disagreement between theory and experiment generalizes to multi-nucleon stripping the problematics of deeply-bound (expensive) nucleon removal from unstable nuclei, abundantly discussed in the literature [6–8, 27].

In summary, we measured inclusive multi-nucleon removal cross sections from ^{112}Sn and ^{104}Sn at ∼150 MeV/nucleon mid-target energy. The removal of identical nucleons from a nucleus shows two distinct regimes, strongly correlated with the evaporation cost asymmetry ΔC of the produced nucleus, with a minor dependence on the projectile or target nature. The correlation appears to be universal according to existing data sets and driven by the excitation energy deposited by the cascade collisions in the remnant nucleus. A state-of-the-art cascade and de-excitation model reproduces well the removal cross sections for the cheap species, but systematically overestimates the removal of the expensive one. The present study generalizes to several-nucleon removal the insufficient treatment of target-projectile excitations in intermediate-energy peripheral collisions of state-of-the-art reaction models. A deeper understanding of nuclear dissipation should improve drastically microscopic predictions of both one-nucleon knockout reactions from exotic nuclei and the production of very exotic nuclei from fragmentation.

The authors are thankful to the RIBF and BigRIPS teams for the stable operation and high intensity of the radioactive ion beam during the experiment. The authors are gratefull to J. Cugnon for enlightening discussions and to J. Benlliure for providing us the numerical values of cross sections published in reference [12]. This work has been supported by the European Research Council through the ERC Starting Grant MINOS-258567 and by the ENSAR european FP7 project number 262010. A. Jungclaus acknowledges support from the Spanish Ministerio de Ciencia e Innovación under contracts FPA2009-13377-C02-02 and FPA2011-29854-C04-01. D. Sohler aknowledges travel support from Hungarian Scientific Research funds (contracts No. K100835 and NN104543).

[1] S. Mondal and R. Shanker, Phys. Rev. A **72**, 052705 (2005).
[2] D. Filges and F. Goldenbaum, Handbook of spallation research, Wiley (2009).
[3] C. Agnor and E. Asphaug, Astr. J. **613**, L157 (2004).
[4] D. Filges *et al.*, Report INDC(NDS)-0530 (2008).
[5] A. Obertelli *et al.*, Phys. Rev. C **73**, 044605 (2006).
[6] A. Gade *et al.*, Phys. Rev. C **77**, 044306 (2008).
[7] F. Flavigny *et al.*, Phys. Rev. Lett. **108**, 252501 (2012).
[8] C. Louchart *et al.*, Phys. Rev. C **83**, 011601(R) (2011).
[9] T. Kubo, Nucl. Instr. Meth. Phys. Res. B **204**, 97 (2003).
[10] T. Ohnishi *et al.*, J. Phys. Soc. Jpn. **77**, 083201 (2008).
[11] D. Perez-Loureiro *et al.*, Phys. Lett. B **703**, 552 (2011).
[12] J. Benlliure *et al.*, Phys. Rev. C **78**, 054605 (2008).
[13] B. Blank *et al.*, Phys. Rev. C **50**, 2398 (1994).
[14] M. Mocko *et al.*, Phys. Rev. C **74**, 054612 (2006).
[15] O.B. Tarasov *et al.*, Phys. Rev. C **87**, 054612 (2013).
[16] T. Enqvist *et al.*, Nucl. Phys. A **686**, 481 (2001).
[17] A. Stolz *et al.*, Phys. Rev. C **65**, 064603 (2002).
[18] P. Moller *et al.*, At. Data Nucl. Data Tables **59**, 185 (1995).

[19] R. Bass, Nucl. Phys. A **231**, 45 (1974).
[20] R. Bass, Lecture Notes in Physics **117**, 281 (1980).
[21] J. P. Dufour *et al.*, Nucl. Phys. A **387**, 157 (1982).
[22] J. Benlliure *et al.*, Nucl. Phys. A **660**, 87 (1999).
[23] A. Boudard *et al.*, Phys. Rev. C **66**, 044615 (2002).
[24] A. Boudard *et al.*, Phys. Rev. C **87**, 014606 (2013).
[25] D. Mancusi, in preparation (2013).
[26] A. Kelić *et al.*, IAEA report INDC(NDC)-0530, 181 (2008).
[27] F. Flavigny *et al.*, Phys. Rev. Lett. **110**, 122503 (2013).